Journal of Power Sources 196 (2011) 4314–4323

Contents lists available at ScienceDirect

Journal of Power Sources

journal homepage: www.elsevier.com/locate/jpowsour

Ammonium based ionic liquids immobilized in large pore zeolites: Encapsulation procedures and proton conduction performance

A. Eguizábal[a], J. Lemus[a], M. Urbiztondo[a], A.M. Moschovi[b], S. Ntais[b], J. Soler[a], M.P. Pina[a,*]

[a] Instituto de Nanociencia de Aragón, Universidad de Zaragoza, Campus Rio Ebro, Edificio I+D, C/Mariano Esquillor, s/n, 50018 Zaragoza, Spain
[b] Foundation for Research and Technology Hellas (FORTH), Institute of Chemical Engineering and High Temperature Chemical Processes (ICE-HT), Stadiou Str, Platani, P.O. Box 1414, 26504 Patras, Greece

ARTICLE INFO

Article history:
Received 2 August 2010
Received in revised form 1 December 2010
Accepted 8 December 2010
Available online 21 December 2010

Keywords:
Ammonium based ionic liquids
Large pore zeolites
Composites
Hybrid membranes
PEMFCs

ABSTRACT

Ammonium based ionic liquids immobilized in Y (FAU framework code) and beta (BEA framework code) type zeolites by different solution methods have been comprehensively characterized for their potential applications as hydrophilic-conducting fillers for PEM. In particular (2-hydroxymethyl) trimethylammonium dimethyl phosphate (IL1) and N,N-dimethyl-N-(2-hydroxyethyl) ammonium bis(trifluoromethanesulfonyl) imide (IL2) encapsulated into commercial NaY (Si/Al = 1.5) and NH_4-BEA (Si/Al = 12.5) type zeolites have been investigated. X-ray diffraction, N_2 physisorption, TGA analysis, ATR–FTIR and Raman spectroscopy techniques have been used to assess about the goodness of the encapsulation procedures. Finally, A.C. impedance spectroscopy measurements of tablets prepared from PVDF/composite (1:9 wt. ratio) were performed in order to evaluate their conduction properties. The conduction properties of the composites as a function of temperature and water partial pressure have been finally chosen as analytical tool to define the best encapsulation procedure and IL/Z composite for PEMFCs applications. A possible conduction mechanism, where synergic-inhibition effects between ILs and H_2O molecules coupled to IL dragging by water desorption take place, is also presented.

1. Introduction

Proton exchange membrane fuel cell (PEMFC) is considered as one promising clean and highly efficient power generation technology in 21st century. Current PEMFC operating at low temperatures (<80 °C) encounters several difficulties, such as CO tolerance, heat rejection, which can be, to a great extent, overcome at higher temperatures (120–150 °C). However, the higher temperature conditions are much more challenging to implement, particularly with regards to the durability of the cell component materials [1]. In this way, ionic liquids (ILs) are very promising components to be used as raw materials in PEMFCs due to their particular properties such as excellent thermal stability, exceptional ionic conductivity, low vapour pressure, and high polarity [2–4]. Furthermore, they are unaffected after mixing with several organic compounds. Typically, they are molten salts of voluminous asymmetric organic cations and inorganic anions. Watanabe and co-workers [5] demonstrated their potential applications in fuel cells under anhydrous conditions due to their electroactivity for H_2 oxidation and O_2 reduction in absence of water. They also exhibit high performance as electrolytes but, at the moment, proton conducting membranes based exclusively on ionic liquids useful for PEMFCs have not been successfully obtained. Several authors [6,7] have proposed their use as proton vehicles (replacing the water role) [8] or directly as liquid electrolytes [9]. The main challenge hindering the use of ionic liquids as proton conductor in PEMFCs is the phase separation process that takes place between the polymer phase and ionic liquid rendering in membranes with poor homogeneity. Due to these limitations, increasing research efforts are being focused in the polymerization of monomeric ionic liquids to obtain ionic liquid polymeric membranes either by cross-linking assisted by ultra violet curing [10–13] or by free radical initiation [14,15] for gas separations or fuel cell applications.

On the other hand, zeolites and related materials have been proposed as alternative materials in ionic conducting membranes for direct methanol fuel cells (DMFC) because of their regular micropores that provide selective separations based on adsorption properties, as well as molecular size and shape effects [16]. Accordingly, they are quite appropriate to reduce fuel crossover phenomena [17]. In addition, their tailored hydrophilic properties coupled to their excellent thermal resistance make them ideal fillers to improve the water uptake properties of ionomeric membranes at temperatures above 150 °C for high temperature proton exchange membrane fuel cells (HTPEMFCs) [18]. Unlike silicates, zeolites (Z) exhibit intrinsic conductivity [19,20], also tunable by cation exchange processes or external functionalization [21]. It

* Corresponding author. Tel.: +34 9761155; fax: +34 9762142.
E-mail address: mapina@unizar.es (M.P. Pina).

0378-7753/$ – see front matter © 2010 Elsevier B.V. All rights reserved.
doi:10.1016/j.jpowsour.2010.12.019

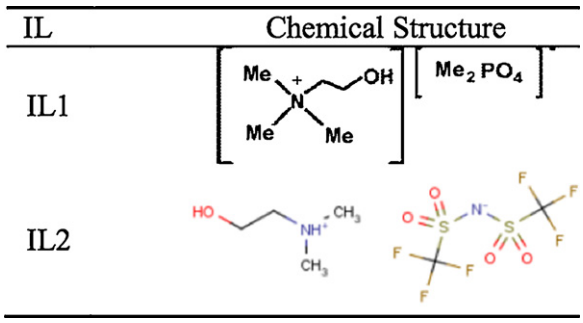

Fig. 1. Chemical structure of the ammonium based ILs used in this work.

has been demonstrated that the acid functionalization of zeolite nanocrystals adds the benefits of increased hydrophilicity and improved proton conductivity in the range of 1.2–12 mS cm^{-1} at room temperature [22].

The combination of zeolites and ionic liquids could result in composite materials (IL/Z) suitable for different applications. As an example, DeCastro et al. [23] immobilized a mixture of 1-butyl-3-methyl-imidazolium chloride and $AlCl_3$ on different porous supports (SiO_2, Al_2O_3, TiO_2, ZrO_2 and H-BEA zeolite) in order to prepare catalysts for the alkylation reactions of aromatic compounds. However, the application of IL/Z here envisioned is related to their use as hydrophilic conducting fillers on PEM for HTPEMFCs. In particular, the encapsulation of ionic liquids inside the framework structure of large pore zeolites has been attempted to improve the proton conductivity of the microporous material itself.

In the first part of this work, the preparation and physicochemical characterization of IL/Z composites prepared from two different ammonium based ILs and two different zeolite hosts by two different methods has been carried out to validate the experimental procedures in terms of zeolite structure preservation and ionic liquid confinement. The second part of the work has been devoted to the evaluation of the proton conduction properties of the as prepared composites in an attempt to identify the most adequate composite to be used as raw material in HTPEMFCs. Special emphasis on the water partial pressure influence on temperature-conductivity dependence has been carried out to explain the maximum in conductivity attained in the 90–140 °C temperature range.

2. Experimental

2.1. Materials

Two types of commercial large pore zeolites were used as ionic liquid hosts: NH_4-BETA (denoted as BEA) supplied by Zeolyst International (Si/Al ratio = 12.5) and zeolite Y in its Na^+ form (denoted as NaY) from Sigma–Aldrich (Si/Al ratio ~ 2.8). As proton conductors, two ionic liquids based on ammonia salts, depicted in Fig. 1, were studied: (2-hydroxymethyl) trimethylammonium dimethyl phosphate (denoted as IL1) purchased from Solvent Innovation-GMBH [24] and N,N-dimethyl-N-(2-hydroxyethyl) ammonium bis(trifluoromethanesulfonyl) imide (denoted as IL2) supplied by Solvionic [25].

2.2. Encapsulation methods

Two different ionic liquid encapsulation methods have been developed. The first one (referred as Method 1) involves the following steps: (i) zeolite evacuation step at 100 °C at 1 mm Hg for 20 min; (ii) preparation of IL solution in a non-polar solvent such as dichloroethane with a 1:9 wt. ratio; (iii) zeolite addition to the IL solution at 1:1 IL/Z wt. ratio; (iv) vigorous stirring at room temperature for 24 h; (v) Soxhlet extraction using methanol to remove the IL excess at solvent reflux temperature (65 °C) for 2 h; and (vi) final drying at 100 °C overnight in an oven. Similarly, for those samples prepared according to Method 2, the following procedure has

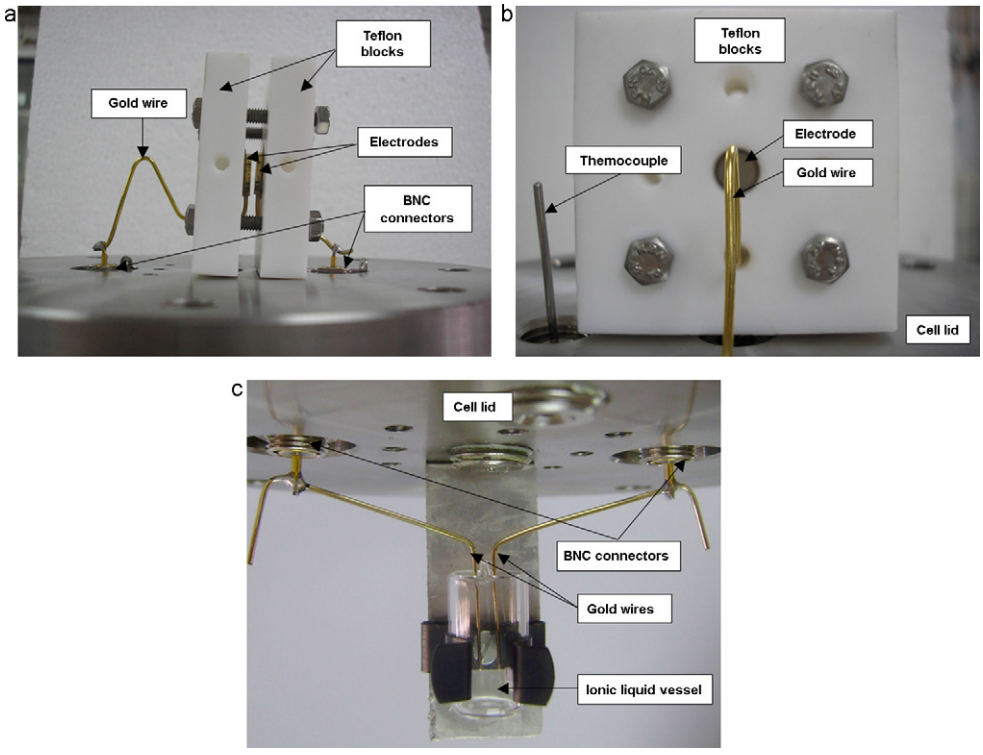

Fig. 2. (a) Upper part of the electrochemical cell lid: tablet sample allocation and electrodes. (b) Upper part of the electrochemical cell lid: tablet sample allocation and control thermocouple. (c) Upper part of the electrochemical cell lid: ionic liquid sample allocation.

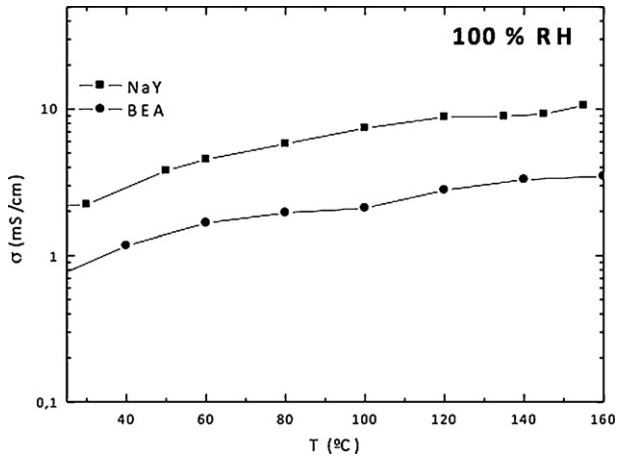

Fig. 3. Proton conductivity of large pore zeolites under saturated conditions.

Table 1
Percentage of mass change after degassing and after water vapours exposure of large pore zeolites (T_{sample} = 120 °C and P_{H_2O} = 4 kPa).

Sample	$\Delta W_{degassing}$ %[a]	$\Delta W_{H_2O\,exposure}$ %[b]
BEA[c]	−9.1	3.2
NaY	−17.1	13.9

[a] The weight change after degassing at 300 °C has been calculated by $(m_{outgassed} - m_0) \times 100/m_0$, where m_0 is the weight recorded for the as prepared sample.
[b] The weight change after vapours exposure has been calculated by $(m_{vapour\ equilibrated} - m_{outgassed,\,80\,°C}) \times 100/m_{outgassed,\,80\,°C}$.
[c] Si/Al ratio = 25.

been used: (i) zeolite crystals outgassing for ∼24 h at 300 °C under vacuum; (ii) preparation of an IL solution in methanol (99.9%); (iii) zeolite powder addition to the IL solution forming suspensions at 2 different IL/Z wt. ratios, namely IL/Z = 1 (standard value), and 1.43; (iv) heating of the suspension at 90 °C overnight for solvent evaporation; and (vi) final drying at 130 °C for ∼8 h. The entire procedure was carried out in a glove bag filled with Ar. In order to remove the excess of the ionic liquid, Soxhlet extraction using methanol as solvent (T = 65 °C) was only performed in the case of IL/Z = 1.43 composite to study its effect on textural and conduction properties. This procedure has been denoted as "Method 2 after Soxhlet" for the remaining of this work.

2.3. Apparatus and measurements

For the proton conductivity characterization of solid samples, all the microporous materials were mechanically mixed with PVDF in 9:1 wt. ratio to ensure enough mechanical resistance. Therefore, tablets 13 mm in diameter were prepared by pressing at 7 ton for 5 min. Afterwards, proton conduction performance was studied by electrochemical impedance spectroscopy (EIS) using an Agilent 4294A Precision Impedance Analyzer (from 40 Hz to 110 MHz as nominal frequency range). However, the frequency operating window was fitted according to the specific sample properties (i.e. composites up to 500 kHz). After obtaining the Nyquist diagram for every test, the resistance value was calculated taking the point in which the semicircle plotted for high frequencies and inclined line for low frequencies intersect each other. The semicircle represents a typical equivalent circuit of a resistor and a capacitor connected in parallel corresponding to the bulk electrical properties, and the line a Warburg impedance caused by the diffusion process of protons [26]. The ionic conductivities were measured in a home-made stainless-steel conductivity cell PTFE lined inside provided with gold electrodes [17] which was immersed in a thermostatic bath. The sample was placed between two electrodes joined with golden wires by tin–silver welding to two thermally resistant and hermetic BNC connectors located in the lid of the cell and coupled to the Impedance Analyzer. Electrodes are also embedded in PTFE blocks hanging from the lid of the cell that are pressed by means of stainless steel screws (see Fig. 2a), to guarantee the electrical contact. In order to ensure an easy and fast water exchange among the chamber atmosphere and the sample (see Fig. 2b), both electrodes were designed ring in shape (11 mm outlet diameter and 6.5 mm inlet diameter). The ionic conductivity of pure ionic liquids was measured in the above electrochemistry cell but changing the ring in shape electrodes by wires placed into a small quartz container for the IL (see Fig. 2c).

Before starting the experiments at 100% RH, the bottom of the cell was filled up with 100 cm^3 of distilled water DDA to attain its vapour pressure once the chamber is closed. On the contrary, for dry conditions, the electrochemical cell previously stored at 80 °C overnight was carefully assembled using dry inert gas to prevent water traces. For the experiments carried out at 4.2 kPa water vapour partial pressure, the electrochemical cell was continuously swept by 10 $cm^3\ min^{-1}$ of N_2 stream saturated with water vapours at room temperature by flowing through a water saturators train.

Thermogravimetric analysis (TGA) of pure ionic liquids and IL/Z composites was performed with a Q5000-IR TGA from TA Instruments, Inc. The samples were heated from room temperature to 650 °C under flow of air with a heating rate 5 °C min^{-1}.

BET surface area and micropore volume were determined by N_2 physisorption measurements using BET equation and t-plot method, respectively. Powder X-ray diffraction (XRD) patterns were obtained on a Bruker D-8 Advanced diffractometer with CuKa X-ray source (40 kV, 40 mA) and equipped with a Lynx Eye position sensitive detector.

Attenuated total reflection infrared (ATR/FTIR) spectra were recorded with a VARIAN EXCALIBUR Coupled with diamond single reflection ATR (Golden Gate of Specac). Finely powdered crystals of both the zeolites and the composites were placed on the sample holder and measured under N_2 flow. FT-Raman spectra were acquired using a Bruker (D) FRA-106/S component attached to an EQUINOX 55 spectrometer. A R510 diode pumped Nd:YAG laser at 1064 nm operating at 250 mW was used for Raman excitation. The powder of the composites or the zeolites was pressed into a stainless steel holder. The spectra were recorded using 4 cm^{-1} resolution and with 800 scans.

Table 2
Water uptake values ($\Delta W_{H_2O\,exposure}$ %) by pure zeolites as a function of temperature and water vapour partial pressures.

P_{H_2O} [kPa]	4.2	4.2	4.2	10
Temperature (°C)	120	150	200	200
BEA[a]	3.6	2.3	1.1	1.3
NaY	13.3	8.8	4.1	5.2

[a] Si/Al ratio = 25.

3. Results and discussion

3.1. Characterization of individual materials: zeolites and ionic liquids

The physico-chemical characterization of the individual materials (i.e. zeolites and ionic liquids) was initially carried out before entrapment experiments. Firstly, TGA measurements were performed onto commercial zeolite powders under presence of water vapours. The samples were first outgassed at 300 °C under Ar and cooled down at 120 °C. The weight increase

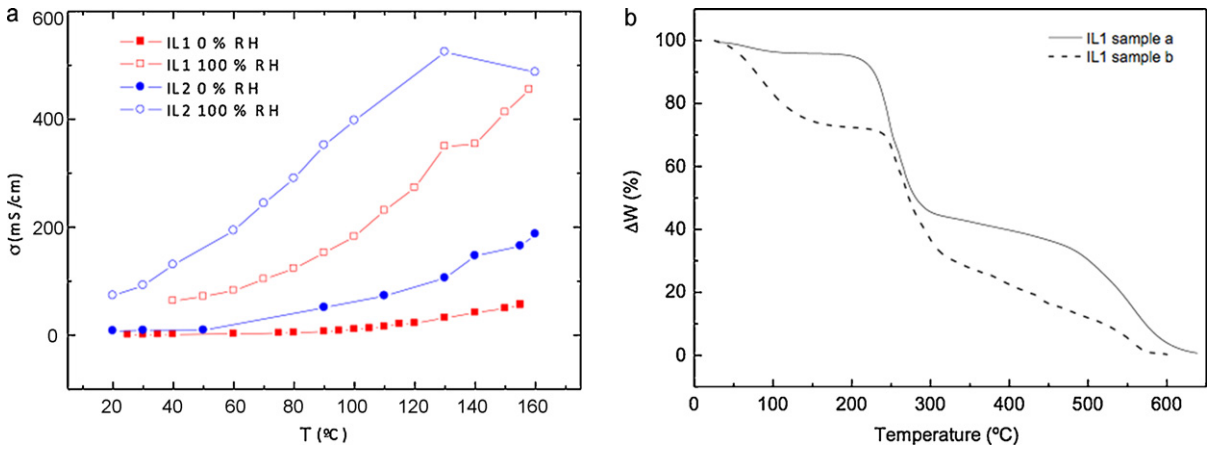

Fig. 4. (a) Proton conductivity of pure ILs under dry and saturated conditions. (b) TGA analyses of IL1 exposed to different atmospheres: sample (a) stored under dry Ar atmosphere, sample (b) exposed at room conditions.

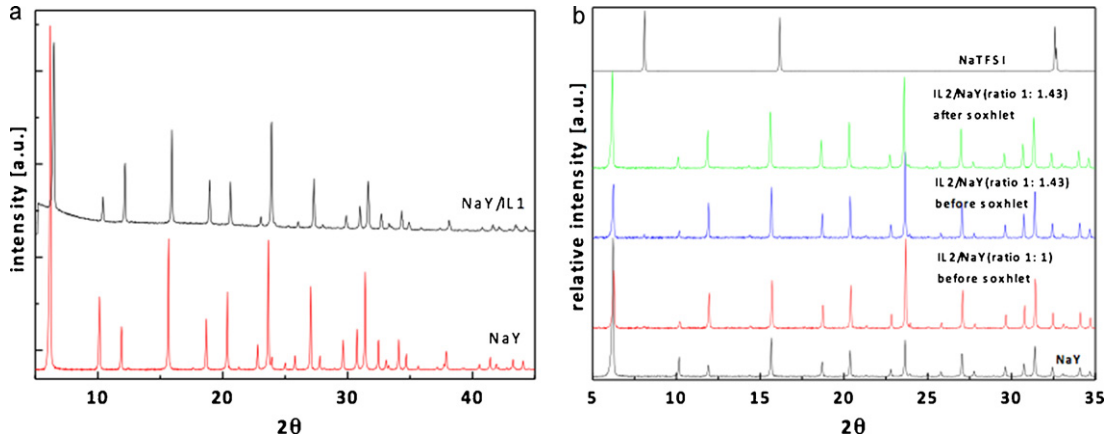

Fig. 5. (a) XRD measurements of the IL1/NaY composite prepared by Method 2. (b) XRD measurements of the IL2/NaY composites with different IL:Z wt. ratios prepared by Method 2 before and after Soxhlet extraction.

was recorded after equilibration with water vapours (P_{H_2O} = 4.2 kPa, in 100 $cm^3\ min^{-1}$ Ar) at 120 °C, 150 °C and at 200 °C. Finally, the sample was kept at 200 °C, the partial pressure of water was increased to ~10 kPa and the weight difference was recorded as well. At all temperatures examined, the amounts of water adsorbed by the NaY crystals were nearly ~4-folds higher than that of the BEA samples (see Tables 1 and 2). It is known that the zeolite hydrophilicity increases with the Al content. Thus, it is expected that NaY (FAU structure) should appear to be more hydrophilic than BEA (BEA structure) counterparts. Table 1 presents the zeolite mass changes after degassing ($\Delta W_{degassing}$%) and after exposure to the water vapours ($\Delta W_{H_2O\ exposure}$%). The weight changes at each

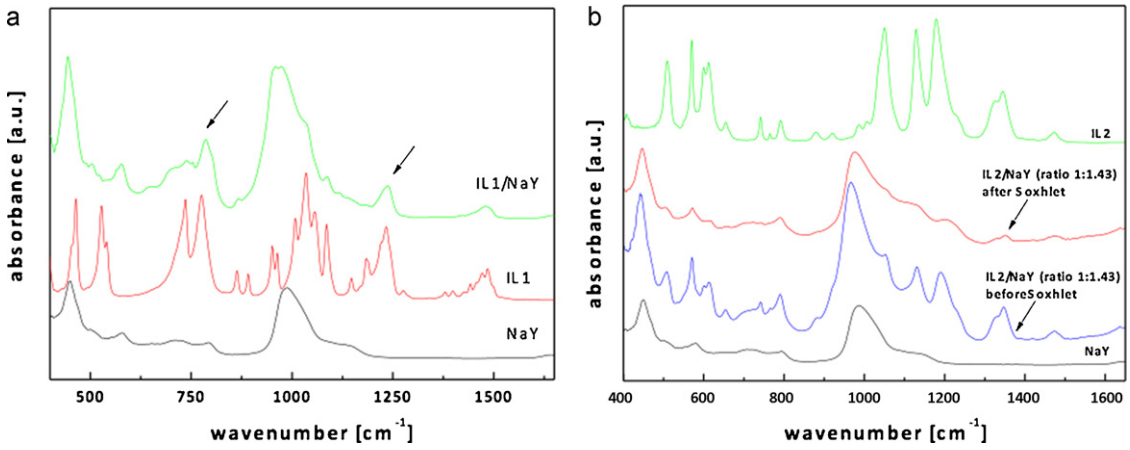

Fig. 6. (a) ATR–FTIR spectra of IL1/NaY composite prepared by Method 2. (b) ATR–FTIR spectra of IL2/NaY composites with high IL:Z wt. ratio prepared by Method 2 before and after Soxhlet extraction.

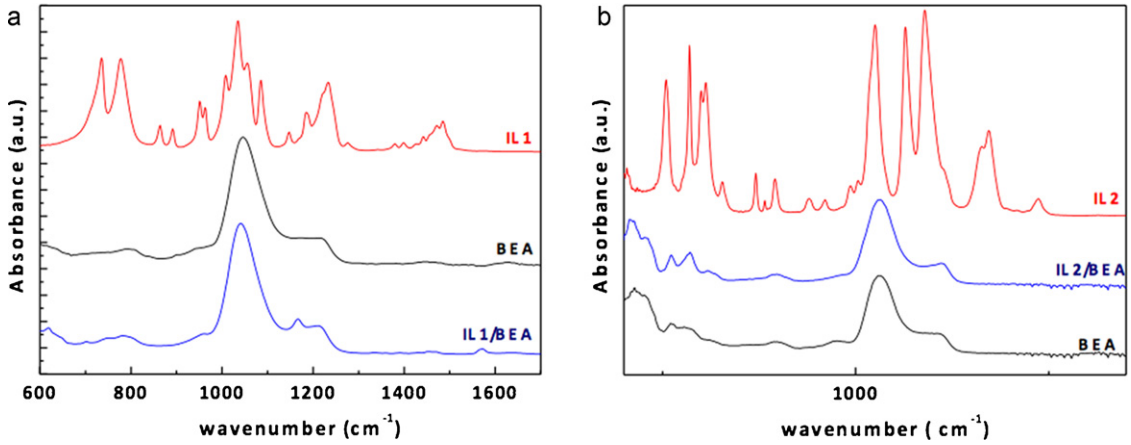

Fig. 7. (a) ATR–FTIR spectra of IL1/BEA composite prepared by Method 1. (b) ATR–FTIR spectra of IL2/BEA composite prepared by Method 2.

temperature reported in Table 2 provide an estimation of the zeolite hydrophilicity and could be used to explain the conduction properties of the as-synthesized powders. The conductivity of the zeolite powders at 100% RH as a function of temperature is shown in Fig. 3. For both zeolites it increases with temperature. However, at all temperatures examined the conductivity of NaY pellets is higher than that of the BEA pellet. If we assume that the differences in the macropore—network characteristics (i.e. porosity, zeolite crystal size and shape) are rather small, then this behaviour could be attributed to the higher water adsorption capacity of zeolite NaY. Hydrophilic zeolites exhibit a higher amount of water molecules (i.e. proton carriers) and also the extra-framework cation solvation degree is superior. This fact leads to a bigger concentration of acceptor sites (δ−) located on the anionic zeolite framework to facilite proton hopping.

Similarly, bulk conductivity measurements of pure ionic liquids under dry (0% RH) and saturated conditions (100% RH) were carried out in the experimental set up depicted in Fig. 2c. The

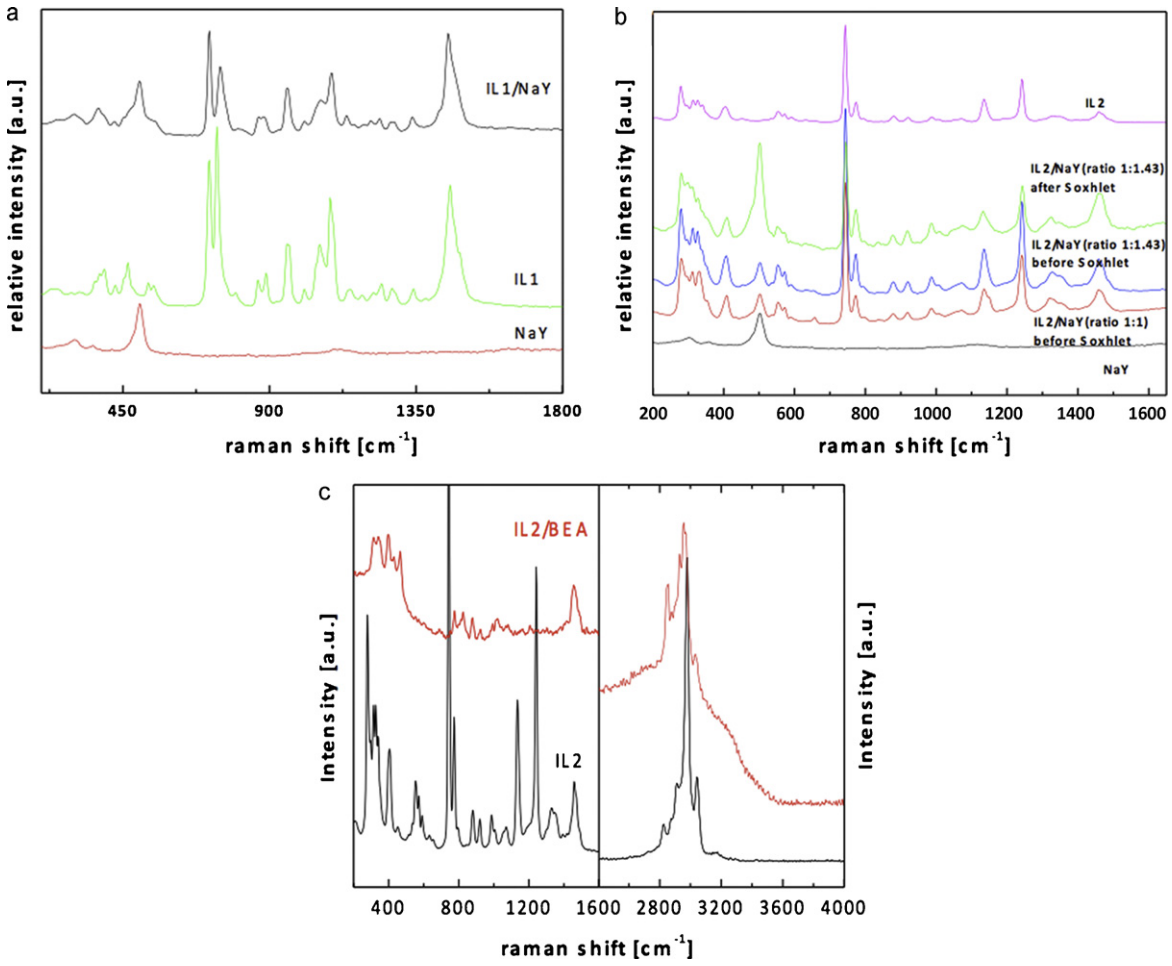

Fig. 8. (a) Raman spectra of IL1/NaY composite prepared by Method 2. (b) Raman spectra of IL2/NaY composites with different IL:Z wt. ratios prepared by Method 2 before and after Soxhlet extraction. (c) Raman spectra of IL2/BEA composite prepared by Method 2.

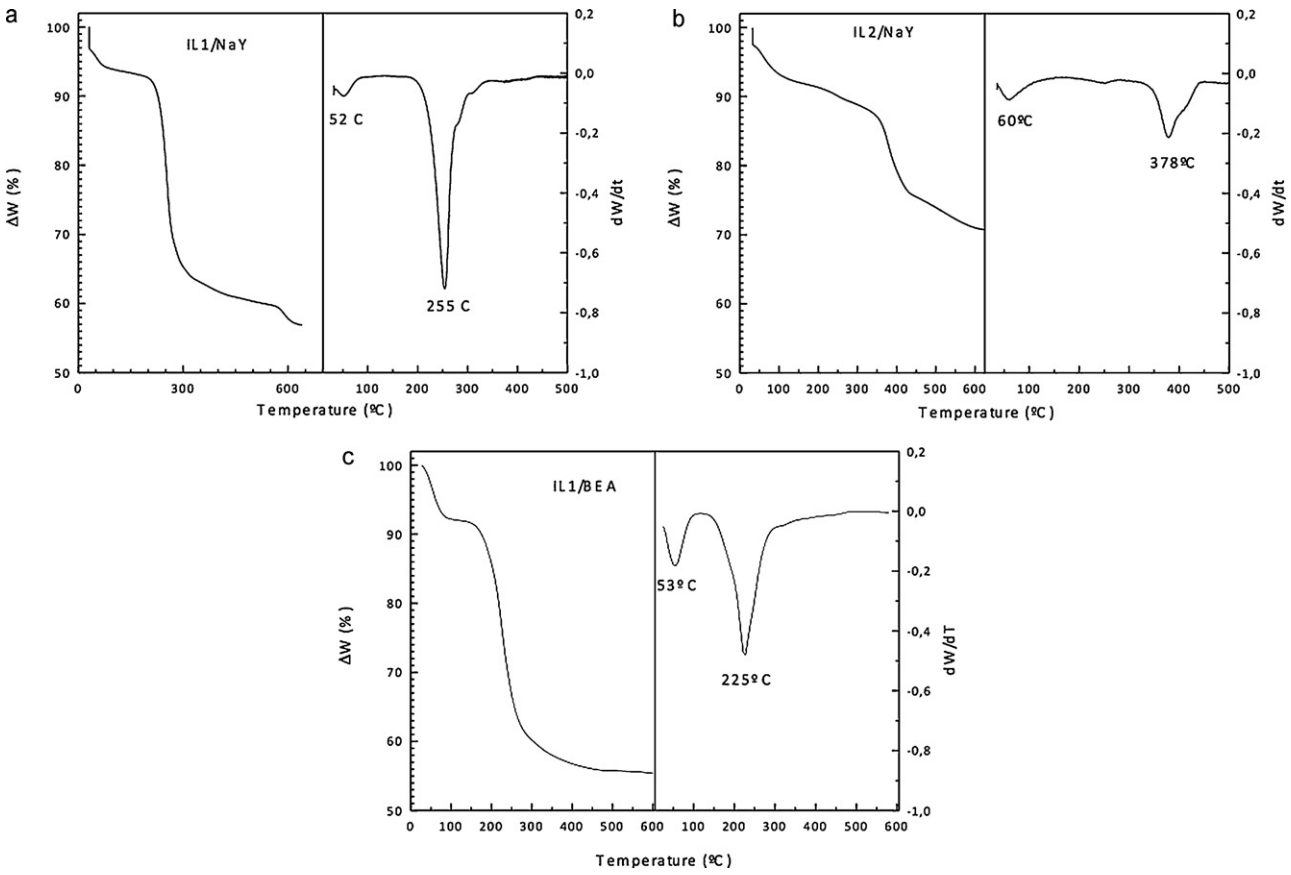

Fig. 9. (a) TGA analysis of IL1/NaY composite prepared by Method 2. (b) TGA analysis of IL2/NaY composite with high IL:Z wt. ratio prepared by Method 2 after Soxhlet extraction. (c) TGA analysis of IL1/BEA composite prepared by Method 1.

Table 3
Textural properties of some of the IL2/NaY composites prepared in this work.

Sample	BET area ($m^2\,g^{-1}$)	Micropore volume ($cm^3\,g^{-1}$)[a]	Micropore area ($m^2\,g^{-1}$)[a]	External surface area ($m^2\,g^{-1}$)[a]
NaY	664	0.25	638	26
IL2/NaY (ratio 1:1) before Soxhlet	1.2	0	0	1.2
IL2/NaY (ratio 1:1.43) after Soxhlet	12.8	0	6.9	5.9

[a] *t*-Plot method.

conductivity measurements as a function of temperature (up to 160 °C) are shown in Fig. 4a. For both ionic liquids, the presence of humidity clearly improved the conduction performance. As an example, the conductivity values of IL1 and IL2 increase ~10- and ~5-fold respectively at 130 °C due to their hydrophilic nature. The hydrophilic nature of the ILs is also evidenced by TGA analysis. As an example, Fig. 4b shows the thermograms of IL1 samples stored in different environments: dry inert atmosphere and room conditions for samples a and b, respectively. As it can be observed, the water uptake value (expressed per initial mass) is nearly 25% for sample b. The estimated decomposition temperature from TGA and DSC (not shown here) analysis are 245 °C

Table 4
Comparison of proton conduction properties of IL/Z composites prepared by method 1.

Sample	σ ($mS\,cm^{-1}$) 60 °C, 100% RH	σ ($mS\,cm^{-1}$) 120 °C, 100% RH	σ ($mS\,cm^{-1}$) 160 °C, 100% RH	σ ($mS\,cm^{-1}$) 60 °C, y_{H_2O} = 5%	σ ($mS\,cm^{-1}$) 120 °C, y_{H_2O} = 5%	σ ($mS\,cm^{-1}$) 160 °C, y_{H_2O} = 5%
NaY	4.5	8.8	10.4	–	–	–
IL1/NaY	24.7	17.1	–	2.8	0.36	0.06
IL2/NaY	20.7	3.4	–	27.9	0.52	0.23
BEA	1.6	2.8	3.4	–	–	–
IL1/BEA	13.3	80.1	30.9	9.4	1.6	2.4
IL2/BEA	23.6	24.9	0.44[a]	0.21	0.09	0.21

[a] Evaluated at 150 °C.

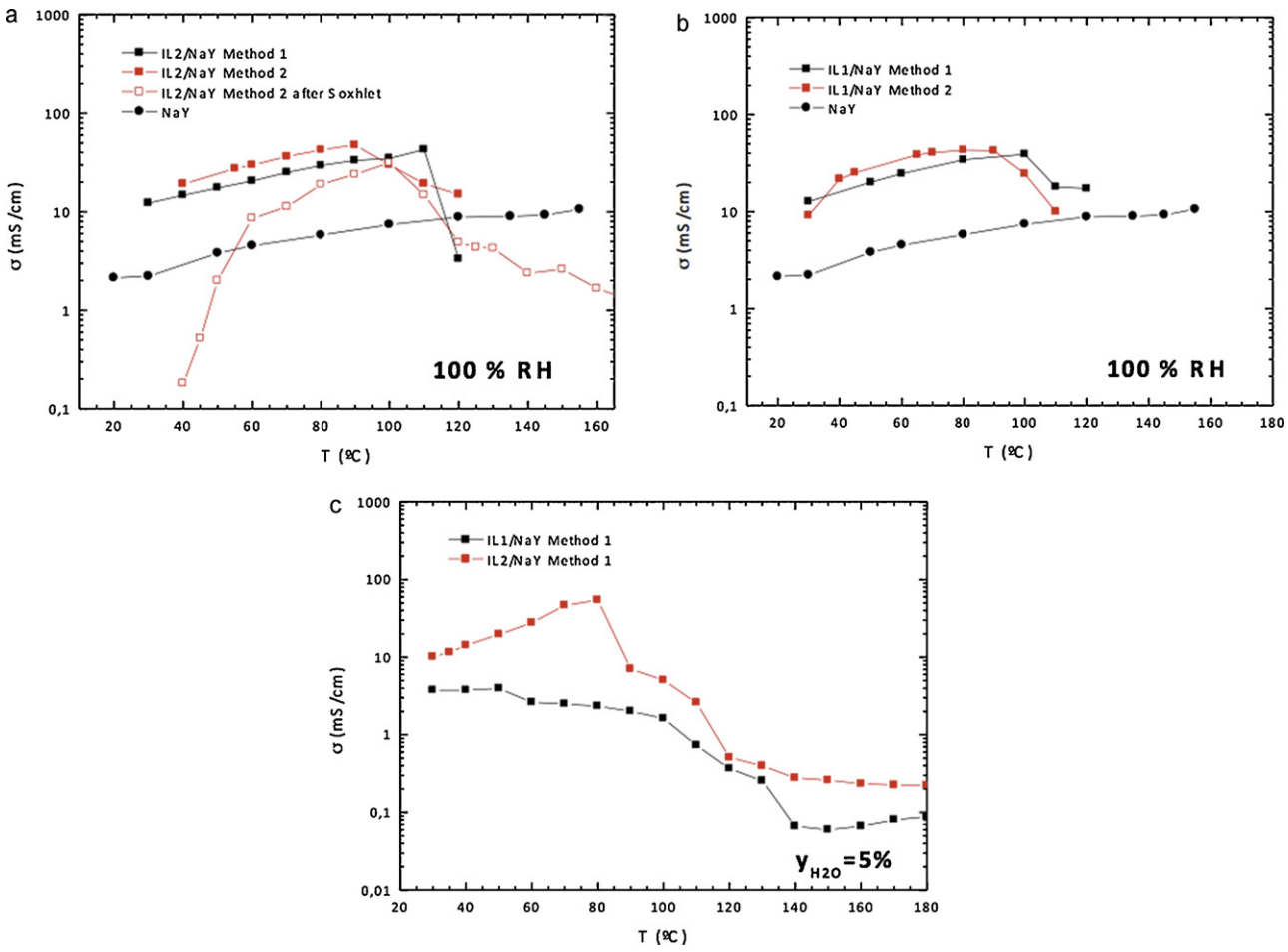

Fig. 10. (a) Conduction performance of IL2/NaY composites prepared by Methods 1 and 2 at saturated conditions. (b) Conduction performance of IL1/NaY composites prepared by Methods 1 and 2 at saturated conditions. (c) Conduction performance of ILs/NaY composites prepared by Method 1 at 4.2 kPa water partial pressure.

and 386 °C for IL1 and IL2 respectively. Accordingly, both ionic liquids exhibit suitable thermal stability for their deployment as proton conductors in HTPEMFCs. Considering the higher conduction performance of IL2 (187 mS cm^{-1} vs. 57 mS cm^{-1} at 160 °C) and the poor stability of dimethyl phosphate anions in presence of water vapours; N,N-dimethyl-N-(2-hydroxyethyl) ammonium bis(trifluoromethanesulfonyl) imide (IL2) seems to be the most promising candidate for encapsulation purposes. However, its higher molecular size, mainly due to the anion volume estimated in 0.44 nm^3 [27], is its main drawback. Therefore, a comprehensive encapsulation study for both ILs has been carried out.

3.2. Characterization of ionic liquid/zeolite composites

XRD measurements of the composite powders obtained after Soxhlet extraction were performed in order to detect any structural changes of the zeolite framework after ionic liquid impregnation. The diffractograms of the IL1/NaY (Fig. 5a) and IL2/NaY (Fig. 5b) composites clearly show the existence of the characteristic peaks of the zeolite revealing that the structure of the zeolite host was not affected by the encapsulation procedures used. The most pronounced changes observed concern the relative intensity of the main diffraction peaks. Similar changes have been reported in the literature for FeII(bpy)$_3$ [28] and for organic [29] and metallorganic complexes [30] entrapped into NaY and they have been attributed to a re-distribution of Na^+ ions into the zeolite crystal. In our case, this change in the relative intensity of the XRD peaks could be due to an ion-exchange reaction that takes place during the entrapment, i.e. the ammonium based cations could replace the extra framework sodium ions. Similar changes have been reported for the NaY zeolite after the encapsulation of H-3-methylimidazolium bis(trifluoromethanesulfonyl) imide [31,32]. The formation of NaTFSI could be ascertained by the XRD spectra of the composite with IL/Z = 1.43 before Soxhlet extraction. New diffraction peaks at $2\theta = 8.1^\circ$ and 16.1° are slightly observed and could be attributed to the formation of sodium bis(trifluoromethanesulfonyl) imide (denoted as NaTFSI in Fig. 5b). The absence of these peaks on the XRD pattern of the same sample after Sohxlet extraction is due to the dissolution of NaTFSI in the extraction solvent. On the contrary, the same analysis was carried out for BEA samples (not shown here), and revealed the absence of these effects; indicating that either NaTFSI might not form or might not be detected by using X-ray diffraction because of the Si/Al ratio in BETA zeolite.

The effect of Soxhlet extraction on the textural properties of selected IL2/NaY composites prepared by Method 2 is shown in Table 3. N_2 physisorption measurements were carried out onto samples outgassed at 200 °C for 3 h under vacuum. Both pore volume and micropore area values tend to zero for the sample before Soxhlet extraction in opposition to the starting NaY zeolite (0.25 cm^3 g^{-1} and 638 m^2 g^{-1}, respectively); whereas a small increase (up to 6.9 m^2 g^{-1}) is observed after Soxhlet extraction. The absence of any microporosity in the sample before Soxhlet extraction can be attributed either to the formation of an IL2 layer on the external surface of the zeolite that essentially blocks the access of N_2 to the "interior" volume of the crystal or to the complete filling

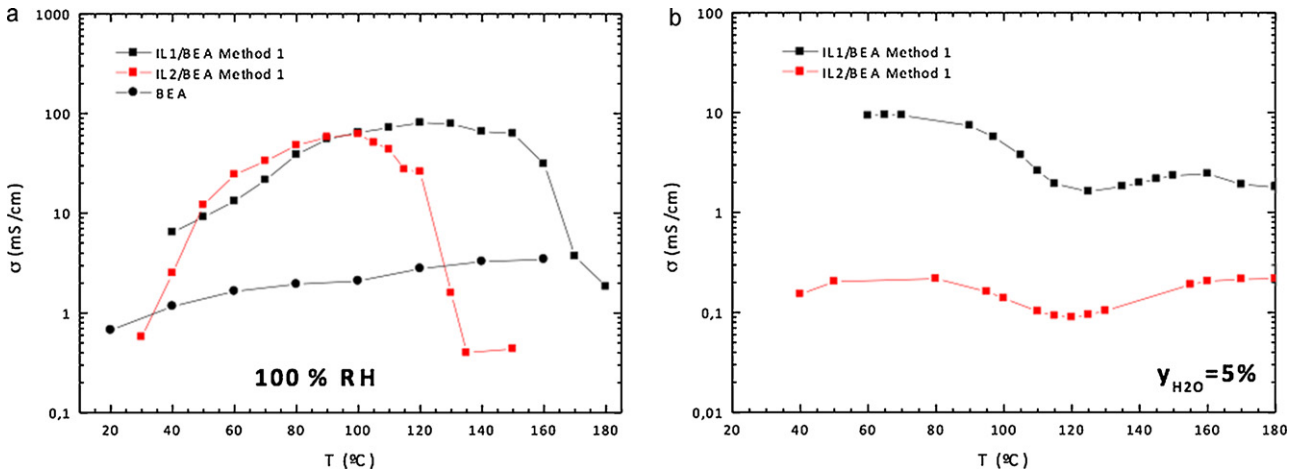

Fig. 11. (a) Conduction performance of ILs/BEA composites prepared by Method 1 at saturated conditions. (b) Conduction performance of ILs/BEA composites prepared by Method 1 at 4.2 kPa water partial pressure.

of the entire zeolite pore volume. If the former explanation was true, then the micropore volume should have abruptly increased after Soxhlet extraction unless a strongly bonding to the external surface of the zeolite crystals took place. Similar studies carried out with H-3 methylimidazolium bis(trifluoromethanesulfonyl) imide-NaY composites [31] prepared from different IL:Z wt. ratios (ranging from 0.03 to 1) could provide us with valuable information to elucidate the location of the guest molecules. For such composites, a gradual decrease of the specific surface area with the IL:Z ratio owing to a progressive pore filling was observed. Therefore, and considering the similarities in both ILs (sharing the same anion), it seems reasonable to postulate a similar behaviour.

ATR–FTIR measurements of IL1/NaY, IL2/NaY, IL1/BEA and IL2/BEA composites are depicted in Figs. 6 and 7, respectively. The spectra of the zeolite powders and ionic liquids have also been included for comparison purposes. In the case of the NaY composites the obtained spectra corroborate the existence of most bands of the pure IL. Moreover, the characteristic FTIR bands assigned to the ILs are more pronounced for those samples not exposed to the final Soxhlet extraction step to remove the IL in excess. It is also worthwhile to underline that the main ILs characteristic bands have very low intensity compared to those characteristics of BEA zeolite. This observation is attributed to the higher IL loadings obtained in the NaY type zeolite (FAU structure) compared to the BEA counterparts, and it is also corroborated by the TGA analyses shown in the section below.

FT-Raman spectroscopy was mainly performed onto NaY based composites (see Fig. 8). They provide information primarily about the ILs, because the Raman scattering of pure zeolites is rather weak. Particularly, the characteristic Raman shift for zeolite NaY is observed around 502 cm^{-1} [33] and is attributed to the T–O–T bending vibration (where T denotes Si or Al atoms). The recorded spectra clearly indicate that ILs have not been completely removed by Soxhlet extraction for both preparation methods used, indicating an effective entrapment inside the zeolite pore network. In general, no relevant changes can be observed in the Raman spectra of composite samples in comparison to those of the pure ILs, although variations in the relative intensities are identified indicating either conformational changes of the voluminous ions inside the zeolite cavities or the formation of NaTFSI due to the extra-framework cation exchange processes [31,32].

In a step further, the final amount of IL entrapped onto the zeolite host has been determined for some of the composites by TGA

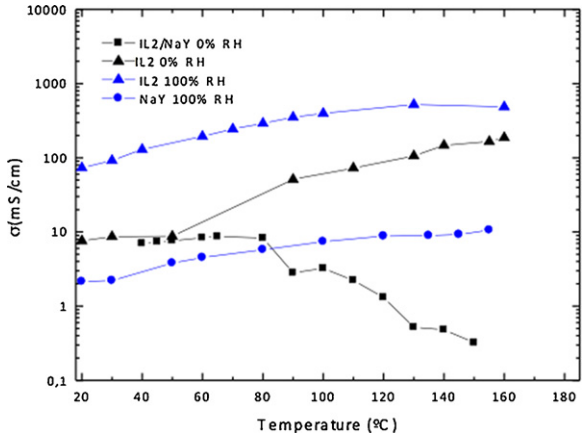

Fig. 12. Conduction performance of IL2/NaY composites prepared by Method 1 as a function of relative humidity.

(see Fig. 9). The differential thermograms have also been depicted to illustrate the water and IL thermal events. From data comparison with TGA of individual materials it could be concluded that, the water uptake values for NaY composites have been reduced due to zeolite pore filling with IL molecules. This effect is more pronounced for IL1/NaY sample (from 17.1% to 10.9%) due to the lower hydrophilicity of IL1. It is also noticeable that ILs decompose in the same temperature range (circa 225–255 °C and 378 °C regions for IL1 and IL2, respectively) when are encapsulated. For the same preparation method and a given zeolite host, the IL1 loadings are always higher than IL2 counterparts (29.3 wt% vs. 17 wt% for NaY composites), in agreement with the lower molecular size of dimethyl phosphate anion. In addition, the zeolite framework seems to have no influence in the case of IL1 (29.3 wt% for NaY vs. 28.8 wt% for BEA composites), but it is relevant for IL2 (17 wt% for NaY vs. 5 wt% for BEA composites). In the later case issues related to the larger size of IL2 might result in lower loadings in BEA due to steric factors.

From the above experimentation it could be concluded that both methods are suitable to encapsulate the ILs preserving at the same time the zeolite framework. In spite of the higher IL loadings attained without Soxhlet extraction, this last preparation step is highly recommended for stability and reproducibility issues.

3.3. Conductivity measurements of ionic liquid–zeolite composites

As N_2 physisorption analysis and TGA are time-consuming to be performed for the whole set of samples prepared, the conduction properties of the composites as a function of temperature and water partial pressure have been finally chosen as analytical tool to define the best encapsulation procedure and IL/Z composite for PEMFCs applications. In all cases, the conductivity for the IL/Z composites is different than that of the individual IL and zeolite materials. The latter shows a conductivity that increases with temperature, while the conductivity of the former passes through a maximum. A possible conduction mechanism, where synergic-inhibition effects between ILs and H_2O molecules coupled to IL dragging by water desorption take place, is proposed below to explain these results.

The conduction performance at saturated conditions of NaY based composites prepared following Methods 1 and 2 is shown in Fig. 10a and b for IL2/NaY and IL1/NaY composites respectively. Method 2 provides better conductivity properties than Method 1 in the low temperature region for a given composite (i.e. 42.5 mS cm^{-1} vs. 29 mS cm^{-1} for IL2/NaY and 42 mS cm^{-1} vs. 34.3 mS cm^{-1} for IL1/NaY at 80 °C) but lower values at high temperatures are obtained (i.e. 19 mS cm^{-1} vs. 42.8 mS cm^{-1} for IL2/NaY and 9.9 mS cm^{-1} vs. 17.5 mS cm^{-1} for IL1/NaY at 110 °C). In order to assess about the real influence of the solvents used for the ILs impregnation, IL excess removal was carried onto IL2/NaY sample prepared by Method 2. This final step means a negative effect on conductivity (i.e. 42.5 mS cm^{-1} before Soxhlet vs. 18.6 mS cm^{-1} after Soxhlet for IL2/NaY at 80 °C), as it could be expected. In spite of this, the extraction step is included in the final preparation protocol for reproducibility and stability reasons. Accordingly with the results, Method 1 (i.e. dichloroethane as IL solvent) seems the most adequate, and therefore it has been systematically used for the remaining conductivity measurements.

For a given preparation conditions and 100%RH, the IL1/NaY composites outperform IL2/NaY counterparts in the low temperature region (34.3 mS cm^{-1} vs. 29 mS cm^{-1} at 80 °C) in spite of the higher conductivity of pure IL2. On the contrary, for experiments carried out at a typically water partial pressures in a PEMFC (y_{H_2O} = 5%), the observed trend (see Fig. 10c) is just the opposite (2.4 mS cm^{-1} for IL1/NaY vs. 50.1 mS cm^{-1} IL2/NaY at 80 °C). These results indicate that conduction performance in the low temperature region is not only due to the IL molecules trapped inside the zeolite framework and competition effects between zeolite and IL for water molecules take place hindering, in some cases, the protons migration. For IL1 (the less hydrophilic material) a beneficial water effect (either as proton vehicle or to promote compensation-cation solvation) is prevailing (i.e. 2.4 mS cm^{-1} vs. 34 mS cm^{-1} at 80 °C and 5% and 100% RH respectively). In a different way, for the hydrophilic and more voluminous IL2, the water inhibition effects are quite notorious (i.e. 52.1 mS cm^{-1} vs. 28.5 mS cm^{-1} at 80 °C for 5% and 100% RH, respectively). In this case, not only the IL2 encapsulated molecules but also the acid zeolite sites are competing for water adsorption inside the heavily traffic zeolite framework, hindering the proton motion through either the solvated IL2 acid–base network or the zeolite framework. When the partial pressure is decreased up to 4.2 kPa (y_{H_2O} = 5%), the water solubility in the IL2 is lower, the competition effects are diminished and as result the overall conductivity increases with respect to the 100% RH in the low temperature region.

The conduction performance of BEA based composites at 100% RH and y_{H_2O} = 5% is shown in Fig. 11a and b, respectively. One of the most remarkable features is that the conductivity decrease occurs at temperatures slightly higher than NaY counterparts (up to 130 °C for IL2/BEA at 100% RH) probably due to the less hydrophilic nature of BEA zeolite (Si/Al ratio = 12.5).

Under saturated conditions, the IL2/BEA composites outperform IL1 based counterparts in the low temperature region (46.5 mS cm^{-1} vs. 36.3 mS cm^{-1} at 80 °C). On the contrary, at temperatures above 100 °C, the behaviour is just the opposite (0.43 mS cm^{-1} vs. 61 mS cm^{-1} at 150 °C). These observations are in agreement with the low IL2 loading values (around 5 wt%), that seem not enough to form a continuous percolating path for proton conduction. In the low temperature region, this effect is hindered by the beneficial water adsorption; but becomes more noticeable as temperature increases. Indeed, the IL2/BEA conductivity at 150 °C is lower than the registered for pure BEA zeolite (3.3 mS cm^{-1} at 150 °C) due to the proton motion is inhibited by isolated IL2 guess molecules. It is worthwhile to mention that under saturated conditions, the performance of IL/BEA composites clearly outperform IL/NaY at temperatures above 100 °C.

When the partial pressure is decreased up to 4.2 kPa (y_{H_2O} = 5%), the IL contribution to the conduction is higher and therefore the filling of the zeolite pores by IL is crucial (9 mS cm^{-1} vs. 0.2 mS cm^{-1} at 80 °C for IL1/BEA and IL2/BEA, respectively). According to Fig. 11b, the amount of IL2 incorporated might be too low to ensure a continuous pathway of IL inside the porous framework. Therefore, the proton IL network is somewhere interrupted and mainly the IL2 molecules are playing the role of zeolite competitors for water adsorption, hindering the solvation of extraframework cations.

To get a better insight of the conductivity pattern decrease at certain temperature values, a conduction experience onto IL2/NaY composite was performed at dry conditions. The obtained results are plotted in Fig. 12, where individual materials have also been depicted for comparison purposes. As it can be observed, at temperatures below 80 °C the conductivity values are intermediate of the values of the individual materials (NaY and IL2). Above 80 °C, the conductivity starts to decrease since IL2 molecules are dragged by the water desorbed molecules. It is reasonable to assume that this dragging effect would be more notorious for the most hydrophilic materials (IL2/NaY). In the case of IL1/BEA composite, the conductivity drops sharply above 150 °C. TGA analyses carried out on pellets used forconductivity measurements (not shown here), corroborate this hypothesis.

From the above experimental conductivity measurements, it could be concluded that the conductivity decay is attributed to the desorption of weakly bounded water molecules capable to ionic liquid dragging. The temperature, at which the conductivity of the composite starts to decrease, depends on the hydrophilicy not only of the zeolitic host but also on the ionic liquid itself. Thus, the higher water uptake values, the lower temperature values at which this effect becomes notorious. Consequently, for BEA samples, the conductivity starts to decay at higher temperatures than NaY (the most hydrophilic zeolite) counterparts (160 °C vs. 90 °C for IL1 based composites at 100% RH). Similarly, for IL1 composites the conductivity starts to decay at higher temperatures than IL2 (the most hydrophilic) counterparts (160 °C vs. 120 °C when encapsulated in BEA type zeolite). Finally, a detailed comparison of conductivity values for all the composites tested is summarized in Table 4. Under saturated conditions, BEA composites outperform NaY ones. In principle, this result could seem a bit contradictory due to the hydrophilic properties of NaY host, but it could be fairly understood when proton conductor molecules trapped in the zeolite cavities are competing for water adsorption with the zeolite framework. Accounting from the results obtained at 4.2 kPa water partial pressure, it could be concluded that IL1/BEA arises at the most adequate for HTPEMFCs applications; whereas IL2/NaY composite is the most promising at temperatures below 100 °C.

4. Conclusions

Two commercial ammonium based ionic liquids have been effectively inmobilized onto commercial NaY (Si/Al = 2.8) and NH_4-BEA (Si/Al = 12.5) large pore zeolites by two different procedures involving the solution of the starting IL. From the physico-chemical characterization results, both methods are suitable to encapsulate the ILs preserving at the same time the zeolite framework. Whatever the ionic liquid encapsulated, the thermal stability of the composites is adequate for their deployment in HT PEMFCs. From the conduction properties evaluation, Method 1 which involves the use of dichloroethane (non polar) as ionic liquid solvent and includes a final Soxhlet extraction for IL excess removal arises as the most adequate.

For the same preparation method and a given zeolite host, the IL1 loadings are always higher than IL2 counterparts as it was expected on the basis of the lower molecular size of dimethyl phosphate anion. Although the zeolite framework seems to have no influence in the case of IL1; it is relevant for IL2 where steric factors limitations in BEA structure occur.

The conduction for all the IL/Z composites, unlike individual IL and zeolite materials showing and activated proton conduction with temperature, exhibit the same pattern: a gradual increase up to a maximum followed by a decrease with temperature. A possible conduction mechanism, where synergic-inhibition effects between both proton conductors (i.e. ILs and H_2O molecules) coupled to ILs dragging by water desorption take place, could explain these results. Thus, the conductivity decay could be attributed to the desorption of weakly bounded water molecules capable to ionic liquid dragging. The temperature, at which the conductivity of the composite starts to decrease, depends on the hydrophilicy not only of the zeolitic host but also on the ionic liquid itself. Thus, the higher water uptake values, the lower temperature values at which this effect becomes notorious.

As a conclusion, in the low-medium temperature region the higher hydrophilic composite, IL2/NaY, exhibits the best conduction performance. On the contrary, IL1/BEA composite is the most promising composite among the tested for HT PEMFCs applications.

Acknowledgements

The authors would like to acknowledge financial support from the European Commission through the FP7 funded program ZEOCELL (Grant Agreement No.: 209481) and Solvionic S.A. Company for IL2 delivery.

References

[1] Q. Li, J.O. Jensen, R.F. Savinell, N.J. Bjerrum, Prog. Polym. Sci. 34 (2009) 449–477.
[2] P. Bonhote, A.P. Dias, N. Papageorgiou, K. Kalyanasundaram, M. Gratzel, Inorg. Chem. 35 (1996) 1168–1178.
[3] J. Fuller, A.C. Breda, R.T. Carlin, J. Electroanal. Chem. 459 (1998) 29–34.
[4] D.R. MacFarlane, P. Meakin, J. Sun, N. Amini, M. Forsyth, J. Phys. Chem. B 103 (1999) 4164–4170.
[5] M.A.B.H. Susan, A. Noda, S. Mitsushima, M. Watanabe, Chem. Commun. (2003) 938–939.
[6] J.S. Lee, T. Nohira, R. Hagiwara, J. Power Sources 171 (2007) 535–539.
[7] H. Ye, J. Huanga, J.J. Xua, N.K.A.C. Kodiweera, J.R.P. Jayakody, S.G. Greenbaumb, J. Power Sources 178 (2008) 651–660.
[8] M. Doyle, S.K. Choi, G. Proulx, J. Electrochem. Soc. 147 (2000) 34–37.
[9] R.F.d. Souza, J.C. Padilha, R.S. Gonçalves, J. Dupont, Electrochem. Commun. 5 (2003) 728–731.
[10] J. Lu, et al., Prog. Polym. Sci. 34 (2009) 431–448.
[11] J.E. Bara, S. Lessmann, C.J. Gabriel, E.S. Hatakeyama, R.D. Noble, D.L. Gin, Ind. Eng. Chem. Res. 46 (2007) 5397–5404.
[12] J.E. Bara, E.S. Hatakeyama, C.J. Gabriel, X. Zeng, S. Lessmann, D.L. Gin, R.D. Noble, J. Membr. Sci. 316 (2008) 186–191.
[13] K.J. Simons, K. Nijmeijer, J.E. Bara, R.D. Noble, M. Wessling, J. Membr. Sci. 360 (2010) 202–209.
[14] S. Washiro, M. Yoshizawa, H. Nakajima, H. Ohno, Polymer 45 (2004) 1577–1582.
[15] H. Nakajima, H. Ohno, Polymer 46 (2005) 11499–11504.
[16] B. Libby, W.H. Smyrl, E.L. Cussler, AIChE J. 49 (4) (2003) 991–1001.
[17] T. Sancho, J. Lemus, M. Urbiztondo, J. Soler, M.P. Pina, Micropor. Mesopor. Mater. 115 (2008) 206–213.
[18] V.M. Vishnyakov, Vacuum 80 (2006) 1053–1065.
[19] U. Simon, M.E. Franke, Micropor. Mesopor. Mater. 41 (2000) 1–36.
[20] T. Sancho, J. Soler, M.P. Pina, J. Power Sources 169 (2007) 92–97.
[21] M.B. Berry, B.E. Libby, K. Rose, K.-H. Hass, R.W. Thompson, Micropor. Mesopor. Mater. 39 (2000) 205–217.
[22] B.A. Holmberg, S-J. Hwang, M.E. Davis, Y. Yan, Micropor. Mesopor. Mater. 80 (2005) 347–356.
[23] C. DeCastro, E. Sauvage, M.H. Valkenberg, W.F. Hölderich, J. Catal. 196 (2000) 86–94.
[24] http://www.solvinn.com.
[25] http://www.solvionic.com.
[26] M. Aparicio, Y. Castro, A. Duran, Solid State Ionics 176 (2005) 333–340.
[27] M. Ue, J. Electrochem. Soc. 141 (1994) 3336–3342.
[28] W.H. Quayle, J.H. Lunsford, Inorg. Chem. 21 (1982) 97–103.
[29] M. Nakayama, J. Yano, K. Nakaoka, K. Ogura, Synth. Met. 138 (2003) 419–422.
[30] A. Kozlov, K. Asakura, Y. Iwasawa, Micropor. Mesopor. Mater. 21 (1998) 571–579.
[31] S. Ntais, A.M. Moschovi, F. Paloukis, S. Neophytides, V.N. Burganos, V. Dracopoulos, V. Nikolakis, J. Power Sources (2010), this issue, doi:10.1016/j.jpowsour.2010.09.061.
[32] S. Ntais, A.M. Moschovi, V. Dracopoulos, V. Nikolakis, ECS Trans. 33 (7) (2010) 41–47.
[33] P.K. Dutta, D.C. Shieh, M. Puri, Zeolites 8 (1988) 306–309.